THE JOURNAL OF BIOLOGICAL CHEMISTRY
Vol. 278, No. 9, Issue of February 28, pp. 7573–7579, 2003
Printed in U.S.A.

The Prefusogenic Intermediate of HIV-1 gp41 Contains Exposed C-peptide Regions*

Received for publication, October 31, 2002
Published, JBC Papers in Press, December 13, 2002, DOI 10.1074/jbc.M211154200

Takumi Koshiba‡ and David C. Chan§

From the Division of Biology, California Institute of Technology, Pasadena, California 91125

The human immunodeficiency virus type 1 (HIV-1) envelope glycoprotein is composed of a complex between the surface subunit gp120, which binds to cellular receptors, and the transmembrane subunit gp41. Upon activation of the envelope glycoprotein by cellular receptors, gp41 undergoes conformational changes that mediate fusion of the viral and cellular membranes. Prior to formation of a fusogenic "trimer-of-hairpins" structure, gp41 transiently adopts a prefusogenic conformation whose structural features are poorly understood. An important approach toward understanding structural conformations of gp41 during HIV-1 entry has been to analyze the structural targets of gp41 inhibitors. We have constructed epitope-tagged versions of 5-Helix, a designed protein that binds to the C-peptide region of gp41 and inhibits HIV-1 membrane fusion. Using these 5-Helix variants, we examined which conformation of gp41 is the target of 5-Helix. We find that although 5-Helix binds poorly to native gp41, it binds strongly to gp41 activated by interaction of the envelope protein with either soluble CD4 or membrane-bound cellular receptors. This preferential interaction with activated gp41 results in the accumulation of 5-Helix on the surface of activated cells. These results strongly suggest that the gp41 prefusogenic intermediate is the target of 5-Helix and that this intermediate has a remarkably "open" structure, with exposed C-peptide regions. These results provide important structural information about this intermediate that should facilitate the development of HIV-1 entry inhibitors and may lead to new vaccine strategies.

Entry of the human immunodeficiency virus type 1 (HIV-1)[1] into host cells is mediated by its envelope glycoprotein, a complex of the receptor-binding subunit gp120 and the transmembrane subunit gp41 (1). gp41 possesses membrane fusion activity and contains an N-terminal fusion peptide followed by two heptad repeat regions termed the N-peptide region and the C-peptide region (see Fig. 1*a*) (1, 2). Upon binding of gp120 to its cellular receptors, CD4 and certain chemokine co-receptors, gp41 undergoes a multi-step structural transition from a native, nonfusogenic conformation to a fusion-active conformation (3–7).

The presumed fusion-active conformation of gp41 is a complex of three helical hairpins, in which each hairpin is formed from an N-peptide helix and an anti-parallel C-peptide helix (see Fig. 1*b*) (8–12). This "trimer-of-hairpins" structure is a six-helix bundle consisting of an internal triple-stranded coiled-coil (three N-peptide helices) with three outer C-peptide helices packed along hydrophobic grooves. In this conformation, the fusion peptide and the transmembrane segment are placed in closed proximity, providing a plausible mechanism for apposition of the target and viral membranes (2, 9).

Synthetic C-peptides potently inhibit gp41-mediated membrane fusion (13–15), and one of these, DP178, binds to a conformation of gp41 activated by interaction of envelope protein with cellular receptors (5). These peptide inhibitors are unlikely to target the trimer-of-hairpins structure, because of its extreme stability and the high effective concentrations of the N- and C-peptide regions within a hairpin. These observations suggest that native gp41 converts to a transiently populated "prehairpin" intermediate prior to formation of the fusogenic trimer-of-hairpins structure (see Fig. 6) (2). Other entry inhibitors, such as IQN17 (16), N(CCG)-gp41 (17), $N36^{Mut(e,g)}$ (18), and 5-Helix (19), may also bind this intermediate, although there is no direct evidence for this hypothesis. An understanding of the structural features of this prefusogenic intermediate is critical because it appears to be an attractive drug target (15, 20). Indeed, clinical trials have demonstrated the efficacy of the C-peptide DP178 (also called T-20) in reducing viral titers in HIV-1-infected patients (21, 22).

5-Helix is a designed, recombinant protein (see Fig. 1, *c* and *d*) that consists of three N-peptide regions and two C-peptide regions (19). This protein is thought to bind the C-peptide region of gp41 and potently inhibits the fusogenic activity of gp41 at nanomolar concentrations. However, it is unknown which conformation of gp41 is the target of 5-Helix. In this study, we designed a tagged 5-Helix protein containing the Myc epitope (EQKLISEEDL) and investigated the target of 5-Helix using a surface co-immunoprecipitation assay. Our results show that 5-Helix binds to HIV-1 gp41 only after gp41-expressing cells come in contact with cellular receptors, resulting in association of 5-Helix on the surface of such cells. These results strongly suggest that 5-Helix binds to the prehairpin intermediate of gp41 and that this intermediate is in an "open" conformation that is accessible to inhibitory compounds.

EXPERIMENTAL PROCEDURES

Cloning and Mutagenesis—The plasmid pMMHa3×Myc was used as a template to amplify three tandem copies of the Myc epitope tag by PCR with primers encoding both 5′ and 3′ *Nde*I sites (for N-terminally tagged versions) and with primers encoding both 5′ and 3′ *Bam*HI sites (for C-terminally tagged versions). The amplified 120-base pair frag-

* This work was supported by National Institutes of Health Grant 7 PO1 GM56552-05 and by a Burroughs Wellcome Fund Career Development Award in Biomedical Sciences. The costs of publication of this article were defrayed in part by the payment of page charges. This article must therefore be hereby marked "*advertisement*" in accordance with 18 U.S.C. Section 1734 solely to indicate this fact.

‡ Postdoctoral fellow of the Japan Society for the Promotion of Science.

§ Bren Scholar. Rita Allen Scholar. To whom correspondence should be addressed: Div. of Biology MC114-96, California Institute of Technology, 1200 East California Blvd., Pasadena, CA 91125. Tel.: 626-395-2670; Fax: 626-395-8826; E-mail: dchan@caltech.edu.

[1] The abbreviations used are: HIV-1, human immunodeficiency virus type 1; PBS, phosphate-buffered saline; sCD4, soluble CD4; Tricine, *N*-[2-hydroxy-1,1-bis(hydroxymethyl)ethyl]glycine.

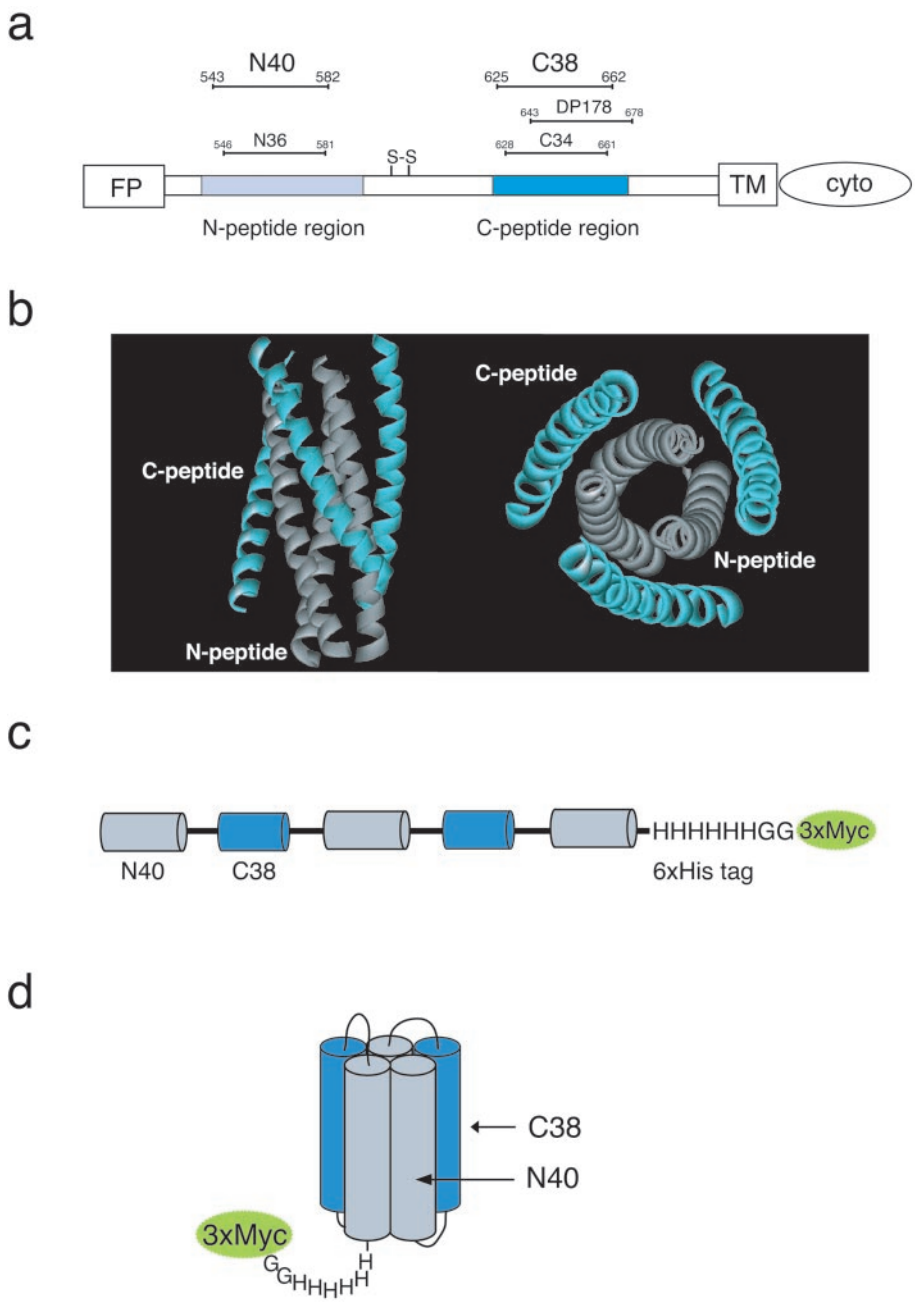

FIG. 1. **HIV-1 gp41 structure and 5-Helix variant.** *a*, a schematic view of HIV-1 gp41, showing the location of the fusion peptide (*FP*), the two hydrophobic heptad repeat regions, the transmembrane segment (*TM*), and the cytoplasmic region (*cyto*). The location of certain N- and C-peptides are drawn above. *b*, a ribbon model of the N36/C34 complex (8), which forms the core of the gp41 ectodomain, viewed looking from the side (*left panel*) and down the 3-fold axis (*right panel*). Molecular graphics were produced using WebLab Viewer (Molecular Simulations). *c*, a 5-Helix variant (5-Helix/3Myc) that consists of three N40 segments (*gray*), two C38 segments (*blue*), a His_6 tag, and a 3Myc epitope tag (*green*). The N40 to C38 junctions are joined with a GGSGG linker, and the C38 to N40 junctions are joined with a GSSGG linker. *d*, a structural model of 5-Helix/3Myc based on the known structure of the N36/C34 complex (8). Note that 5-Helix and its variants lack the third C-peptide helix and therefore bind to free C-peptide with high affinity.

ments were ligated into the p5-Helix plasmid to generate p3Myc/5-Helix and p5-Helix/3Myc, respectively. Aspartate substitutions (V549D, L556D, Q563D, and V570D) in p5-Helix/3Myc were introduced individually into the final (third) N40 segment by PCR to generate p5-Helix(D4)/3Myc. The p3Myc/6-Helix and p6-Helix/3Myc constructs were prepared in the same manner as above by ligating the PCR products into p6-Helix.

Protein Expression and Purification—All of the proteins were expressed in the *Escherichia coli* strain BL21(DE3)/pLysS using the T7 expression system (23). Overnight cultures (10 ml) were used to inoculate 1 liter of Luria Broth medium and grown to log phase at 37 °C. Overproduction of the protein was induced by the addition of isopropyl thio-β-D-galactoside to a final concentration of 1 mM. After 3 h of induction, the cells were harvested and stored frozen (−20 °C) until purification. Bacterial pellets were resuspended in 50 mM Tris-HCl buffer (pH 8.0) containing 100 mM NaCl, lysed by sonication, and centrifuged (6,000 × *g* for 30 min) to obtain an inclusion body fraction. Each 5-Helix and 6-Helix variant was enriched in this fraction. The pellets were resuspended in 100 mM Tris-HCl buffer (pH 8.0) containing 6 M guanidine hydrochloride, 10 mM imidazole, and 1 mM dithiothreitol. After clarification by centrifugation (15,000 × *g* for 15 min), the histidine-tagged proteins were affinity-purified on nickel-nitrilotriacetate (Qiagen) columns at room temperature. The proteins were eluted with 50 mM Tris-HCl buffer (pH 8.0) containing 6 M urea, 100 mM NaCl, and 100 mM imidazole. The eluted protein was refolded by dialyzing against 50 mM Tris-HCl (pH 8.0). After dialysis, all of the proteins were purified to >95% purity by anion exchange chromatography on an ÄKTA Purifier 10 (Amersham Biosciences), using a MonoQ column and a linear gradient of NaCl (0–1 M). Protein concentrations were determined by absorbance at 280 nm in 6 M guanidine hydrochloride (24).

CD Spectroscopy—CD measurements were performed in PBS (pH 7.4) with an Aviv 62DS CD spectrometer (Aviv Associates) equipped with a thermoelectric temperature controller. Wavelength scans (200–260 nm) were performed on 10 μM protein solutions. Thermal denaturation profiles were obtained by measuring the ellipticity at 222 nm (θ_{222}) as a function of temperature. Protein solutions (10 μM) were measured at 1-degree intervals starting at 4 °C, with an equilibration time of 2 min and an acquisition time of 0.5 min. The apparent melting temperature (T_m) was estimated from the maximum of the first derivative of θ_{222} with respect to temperature. Because of the extreme thermal stability of these proteins, these experiments were performed in PBS in the presence of 3.7 M guanidine hydrochloride.

Tissue Culture—NIH3T3 and 293T cell lines were maintained in Dulbecco's modified Eagle's medium supplemented with 1% glutamine,

1% penicillin-streptomycin, and 10% fetal calf serum or 10% bovine calf serum, respectively, at 5% CO_2 and 37 °C. Syncytia assays were performed as described previously (15).

For the cell surface co-immunoprecipitation assays, 2 μg of the HIV-1 envelope expression plasmid pCMVgp160 was transfected by the calcium phosphate method into 2×10^5 293T cells/well in a six-well dish. Two days after transfection, the 293T cells were incubated with 100 μg of each protein in the presence or absence of receptors (10 μg of sCD4 or 3×10^6 target cells) at 37 °C for 1 h. The cells were then washed with PBS (pH 7.4) and lysed with 1.5 ml of lysis buffer (50 mM Tris-HCl, pH 7.4, 150 mM NaCl, and 1% Triton X-100). The clarified supernatants were incubated overnight (4 °C) with 25 μl of Sepharose beads coupled to the anti-Myc monoclonal antibody 9E10. After four washes with PBS, the immunoprecipitates were separated by 10% SDS-polyacrylamide gel electrophoresis and immunoblotted with the anti-gp41 monoclonal antibody Chessie 8 (National Institutes of Health AIDS Research and Reference Reagent Program), and a horseradish peroxidase-conjugated anti-mouse IgG antibody (Jackson ImmunoResearch). To detect binding of 5- or 6-Helix to the cells, the immunoprecipitates were separated on a 12% SDS-polyacrylamide gel and immunoblotted with monoclonal antibody 9E10. The sCD4 and target cell lines (3T3.T4, 3T3.T4.CCR5, 3T3.T4.CXCR4) were obtained from the National Institutes of Health AIDS Research and Reference Reagent Program.

C34 Peptide Binding Assay—The C34 peptide precipitation experiment was performed in 500 μl of PBS (pH 7.4) with 10 μM protein (5-Helix or 6-Helix variants) and 10 μM C34 peptide. The solution was added to 25 μl of anti-Myc beads and incubated at 4 °C for 1 h. After the unbound supernatant was removed, the beads were washed four times with 1.5 ml of PBS buffer. The bead-bound samples were analyzed by a 16.5% Tris-Tricine polyacrylamide gel (25) and immunoblotted with an

TABLE I

Biophysical data and inhibitory potency of 5- and 6-helix variants

CD scans were performed on 10 μM protein solutions in PBS (pH 7.4). For the 3Myc-tagged proteins, the residues of the epitope tag were assumed to be nonhelical and were not included in calculating the molar ellipticity at 222 nm (θ_{222}). The apparent melting temperatures (T_m) were estimated from thermal denaturation profiles of θ_{222}. Inhibition of cell-cell fusion was measured in a syncytium assay. The means and standard errors were calculated from triplicate experiments.

Protein	θ_{222}	T_m	IC_{50}
	deg cm²/dmol	*°C*	*μM*
5-Helix	−28,900	98	0.015 ± 0.002
3Myc/5-Helix	−29,100	98	0.111 ± 0.004
5-Helix/3Myc	−29,100	98	0.046 ± 0.003
5-Helix(D4)/3Myc	−28,200	96	>10
6-Helix	−30,800	>100	>10
3Myc/6-Helix	−30,500	>100	>10
6-Helix/3Myc	−30,600	>100	>10

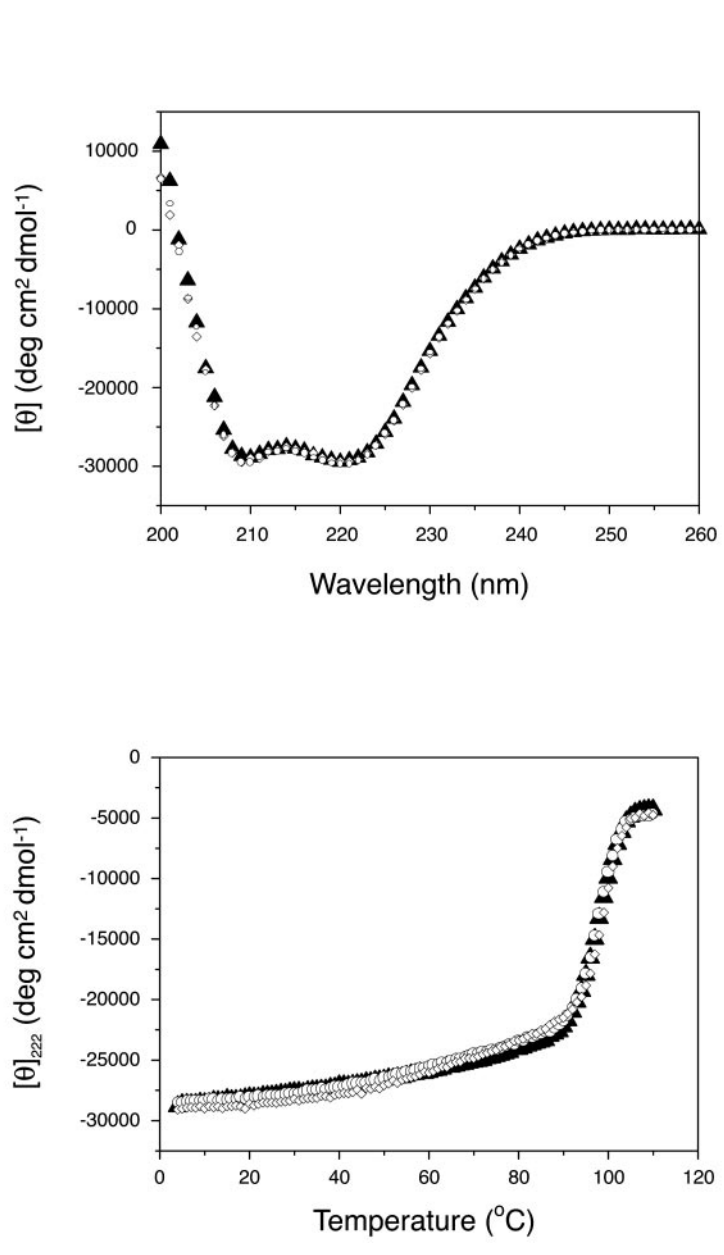

FIG. 2. **Helical structure and thermal stability of 5-Helix variants.** *a*, CD spectra of 5-Helix (▲), 3Myc/5-Helix (◇), and 5-Helix/3Myc (○) at 4 °C in PBS (pH 7.4). *b*, thermal denaturation profiles of 5-Helix (▲), 3Myc/5-Helix (◇), and 5-Helix/3Myc (○) monitored by ellipticity at 222 nm in PBS (pH 7.4) containing 3.7 M guanidine hydrochloride.

anti-C34 polyclonal antibody and horseradish peroxidase-conjugated anti-rabbit IgG antibody (Jackson ImmunoResearch).

RESULTS

Biophysical Characterization of 5- and 6-Helix Variants—To use 5-Helix as a structural probe for gp41, we designed two 5-Helix variants containing three copies of the Myc epitope (EQKLISEEDL) at either the N terminus (3Myc/5-Helix) or the C terminus (5-Helix/3Myc; Fig. 1, *c* and *d*). As a negative control, we constructed a Myc-tagged version of a mutant 5-Helix (5-Helix(D4)/3Myc) that contains a disruption of the C-peptide-binding site and that was previously shown to be ineffective in inhibiting gp41-mediated fusion (19). We also constructed N- and C-terminally Myc-tagged versions of 6-Helix (3Myc/6-Helix and 6-Helix/3Myc, respectively), a protein that does not inhibit HIV-1 membrane fusion because the C-peptide-binding site has been filled by an attached C-peptide.

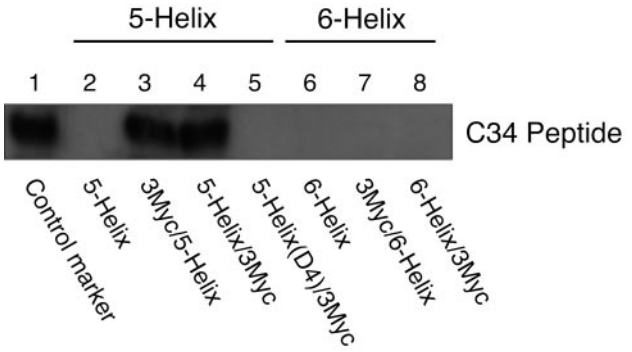

FIG. 3. **C34 peptide binding assay of the 5- and 6-Helix variants.** C34 peptide was mixed with the 5- and 6-Helix variants and immunoprecipitated with an anti-Myc monoclonal antibody. Binding to C34 peptide was determined by Western blot analysis with an anti-C34 polyclonal antibody.

Our two Myc-tagged versions of 5-Helix have biophysical properties nearly identical to untagged 5-Helix (Table I and Fig. 2). By CD analysis, all three proteins show CD spectra with minima at 208 and 222 nm, as is typical for helical proteins (Fig. 2*a*). The molar ellipticities at 222 nm for each of these proteins were indistinguishable, indicating similar levels of helicity (Table I). Moreover, the three proteins were highly soluble (data not shown) and extremely stable, with a melting temperature (T_m) of 98 °C in the presence of 3.7 M guanidine hydrochloride in PBS (pH 7.4) (Table I and Fig. 2*b*). We thus conclude that the Myc epitope tags do not affect the overall helical structure and stability of 5-Helix protein. Likewise, the biophysical properties of 6-Helix/3Myc and 3Myc/6-Helix were nearly identical to untagged 6-Helix. Consistent with previous results, the mutant construct 5-Helix(D4)/3Myc was slightly less helical and less stable than wild-type 5-Helix (Table I) (19).

Inhibitory Activity of 5- and 6-Helix Variants—Both 3Myc/5-Helix and 5-Helix/3Myc bound to synthetic C34 peptide in an immunoprecipitation assay using the anti-Myc monoclonal an-

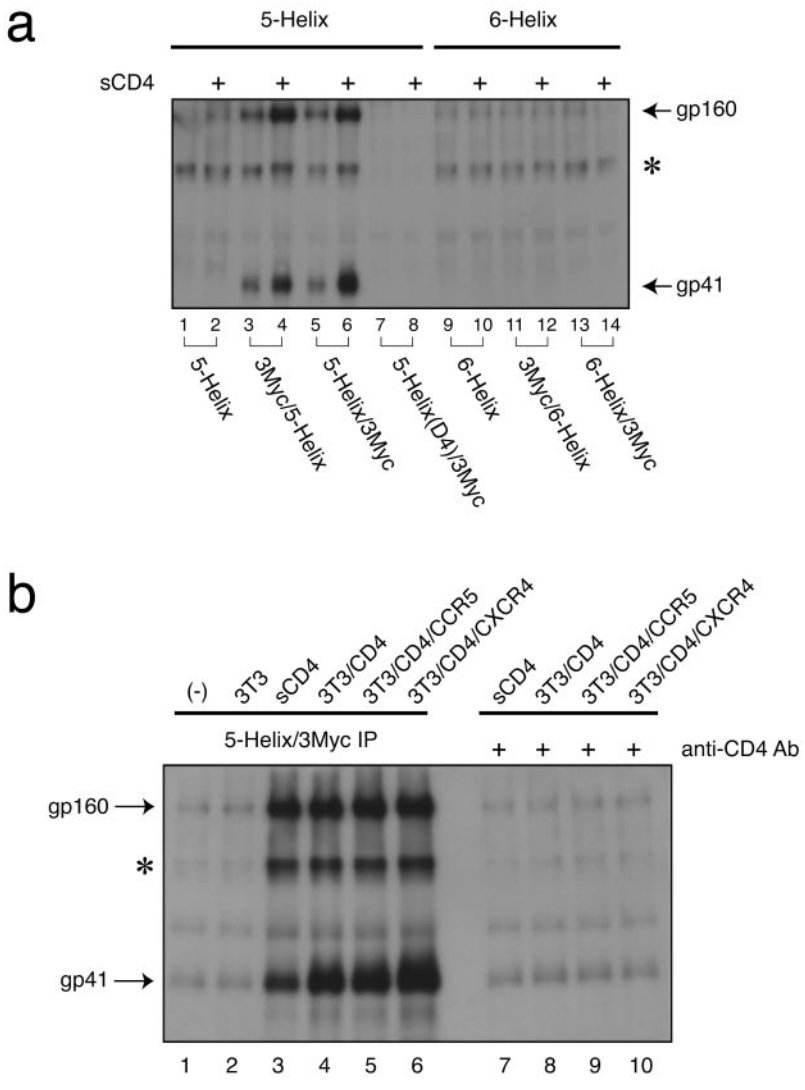

FIG. 4. **Cell surface co-immunoprecipitation of 5- and 6-Helix variants.** *a*, 293T cells transfected with gp160 were incubated with 5-Helix (*lanes 1–8*) and 6-Helix (*lanes 9–14*) variants in the absence or presence of sCD4 and subjected to cell surface co-immunoprecipitation with the anti-Myc monoclonal antibody 9E10. Binding to gp41 was determined by Western blot analysis with the gp41 monoclonal antibody Chessie 8. *b*, 293T cells expressing gp160 were incubated with 5-Helix/3Myc in the absence or in the presence of retrovirally transduced NIH3T3 cell lines that express cellular receptors for HIV-1. Binding to gp41 was determined as in *a*. In *lanes 7–10*, the anti-CD4 monoclonal antibody Q4120 was added to the reactions to block CD4 interactions with gp120. The *arrows* indicate the positions of gp41 and gp160. The background band (*) at ~80 kDa is unrelated to gp120/gp41, as explained in the text.

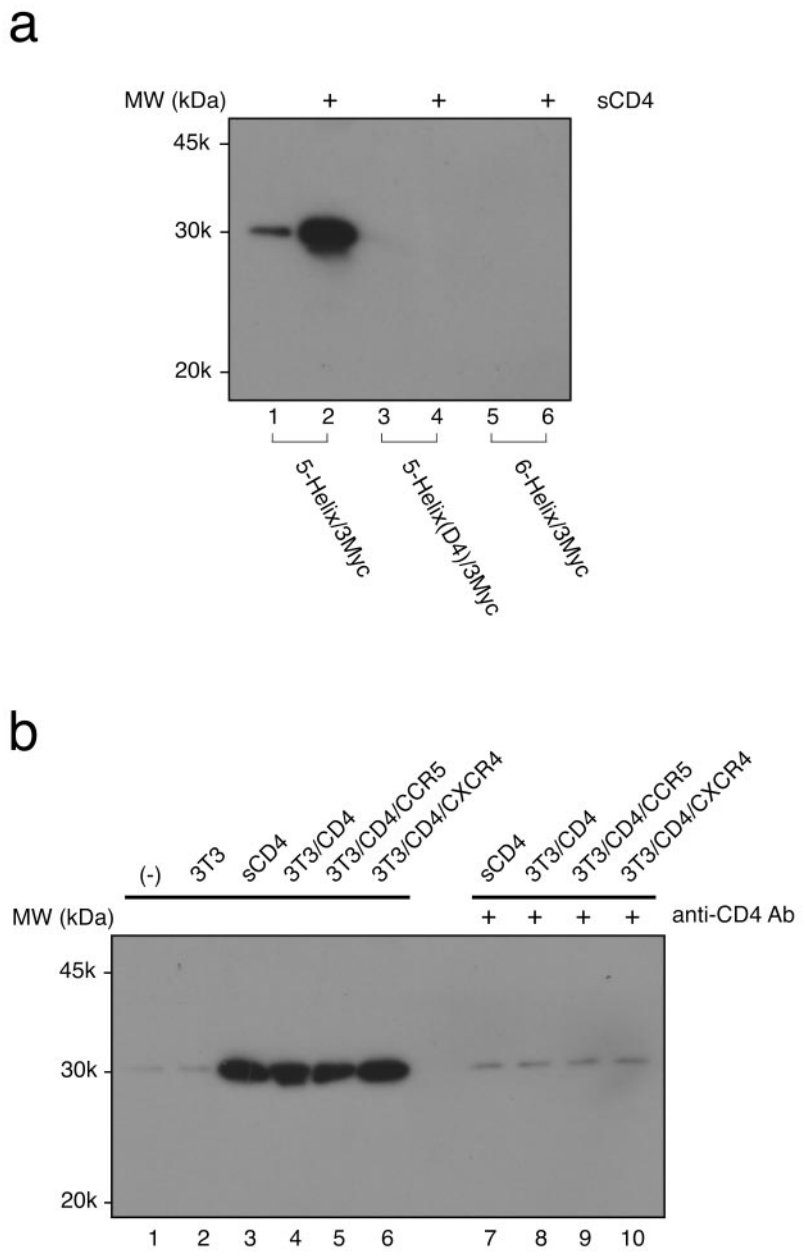

FIG. 5. **Cell surface localization of 5- and 6-Helix variants.** *a*, 293T cells transfected with gp160 were incubated with 5- (*lanes 1–4*) and 6-Helix (*lanes 5* and *6*) variants in the absence or presence of sCD4 and subjected to cell surface immunoprecipitation with the anti-Myc monoclonal antibody 9E10. Association of the protein to the transfected cell surface was determined by Western blot analysis with the anti-Myc monoclonal antibody 9E10. *b*, 293T cells expressing gp160 were incubated with 5-Helix/3Myc in the absence or in the presence of retrovirally transduced NIH3T3 cell lines that express cellular receptors for HIV-1. Association of the protein to the cell surface was determined as in *a*. In *lanes 7–10*, the anti-CD4 monoclonal antibody Q4120 was added to block CD4 interactions with gp120. The positions of protein molecular mass markers are indicated at the *left*.

tibody 9E10 (Fig. 3, *lanes 3* and *4*). In contrast, the 5-Helix(D4)/3Myc, 3Myc/6-Helix, and 6-Helix/3Myc proteins showed no C34 binding (*lanes 5*, *7*, and *8*).

Consistent with their C34 binding activity, both 3Myc/5-Helix and 5-Helix/3Myc showed potent inhibitory activity against cell-cell fusion mediated by HIV-1 envelope protein, with half-maximal inhibition at 111 and 46 nM, respectively (Table I). These values are ~10- and 3-fold less potent than that of untagged 5-Helix. The reduced potency of the tagged proteins may be due to steric constraints in accessing the gp41 C-peptide region during the membrane fusion process. Furthermore, these constraints may be more severe for 3Myc/5-Helix, in which the 39 additional residues of the epitope tag are expected to be oriented toward the viral membrane (see Fig. 6). A reduction in inhibitory activity has also been observed for a hemagglutinin epitope-tagged version of the C-peptide DP178 (5). In contrast to the inhibitory activity of the 5-Helix variants, four different control proteins (5-Helix(D4)/3Myc, 6-Helix, 3Myc/6-Helix, and 6-Helix/3Myc) showed no detectable inhibitory activity at the highest concentration tested (10 μM).

Binding of Tagged 5-Helix to Activated gp41—The preservation of inhibitory activity in 3Myc/5-Helix and 5-Helix/3Myc allowed us to explore the conditions under which 5-Helix binds to gp41. Using a surface co-immunoprecipitation assay, we investigated whether these proteins could bind to gp41 expressed on the surface of transfected 293T cells (Fig. 4*a*). 293T cells were transfected with a HXB2 envelope expression plasmid, which directs expression of gp160, the precursor polypeptide that is proteolytically processed to generate the envelope complex of gp120 and gp41 (26). 48 h after transfection, 293T cells were incubated with the panel of 5-Helix and 6-Helix variants in the presence or absence of sCD4. Binding of these polypeptides to the surface of transfected cells was determined by immunoprecipitation with the anti-Myc monoclonal antibody 9E10. Both 3Myc/5-Helix and 5-Helix/3Myc showed low levels of gp41 binding in the absence of sCD4, and this binding was greatly increased in the presence of sCD4 (*lanes 4* and *6*). The specificity of this gp41 binding was shown by the lack of binding by 5-Helix(D4)/3Myc, 3Myc/6-Helix, and 6-Helix/3Myc (*lanes 8*, *12*, and *14*). Interestingly, a high molecular weight

band, corresponding in size to uncleaved gp160, was also immunoprecipitated in a parallel pattern. Reprobing of the Western blots with an anti-gp120 antibody confirmed that this band was indeed gp160 (data not shown). Because the C-peptide DP178 also has been shown to bind to receptor-activated gp160 (5), this result indicates that significant conformational changes can be induced in the envelope protein even in the absence of proteolytic processing. In these immunoprecipitation experiments, we also detected an 80-kDa background band whose identity is unknown. However, this band is unrelated to HIV-1 envelope, because we also detect it in immunoprecipitations from untransfected 293T cells (data not shown).

We further investigated whether surface-expressed cellular receptors could similarly activate the binding of 5-Helix to gp41. 293T cells expressing gp160 were incubated with 5-Helix/3Myc in the presence of a panel of retrovirally transduced NIH3T3 cell lines that express cellular receptors for HIV-1 (Fig. 4*b*). Whereas nonexpressing NIH3T3 cells showed no effect (compare *lanes 1* and *2*), cell lines expressing CD4 triggered a large increase in binding of 5-Helix/3Myc to gp41 (*lanes 4–6*). The conformational changes allowing binding of 5-Helix/3Myc appear to be largely induced by CD4, because the additional expression of CXCR4 (*lane 6*), the co-receptor for the envelope protein (HXB2 strain) used in these studies, caused only a slight increase in binding. In all cases, the binding of gp41 by 5-Helix/3Myc was effectively inhibited by the monoclonal antibody Q4120 (*lanes 7–10*), which binds to CD4 and blocks its binding by gp120. These results demonstrate that 5-Helix binds to a conformation of gp41 activated by interaction of the envelope protein with cellular receptors.

Association of Tagged 5-Helix on the Surface of Transfected 293T Cells—To further characterize our surface immunoprecipitation experiments, we determined the levels of 5-Helix/3Myc immunoprecipitated from the cell surface in the presence and absence of receptors. Low levels of 5-Helix/3Myc were precipitated in the absence of sCD4 (Fig. 5*a*, *lane 1*), but the levels were dramatically increased in the presence of sCD4 (*lane 2*). In contrast, 5-Helix(D4)/3Myc and 6-Helix/3Myc showed no precipitation either in the presence or absence of sCD4 (*lanes 3–6*).

The level of 5-Helix/3Myc precipitated was not affected by the addition of NIH3T3 cells lacking human HIV-1 receptors (Fig. 5*b*, *lanes 1* and *2*). In contrast, the levels of precipitated 5-Helix/3myc were greatly enhanced by the addition of cell lines expressing CD4 or CD4 and co-receptors (*lanes 4–6*). In all cases, the immunoprecipitation of 5-Helix/3Myc was drastically decreased by addition of the anti-CD4 antibody (Q4120) (*lanes 7–10*), paralleling the trend seen in gp41 binding experiments (Fig. 4*b*). Together these results show that interaction of envelope protein to CD4 facilitates association of 5-Helix to the cell surface.

DISCUSSION

Our results show that 5-Helix binds poorly to native gp41 but well to gp41 activated by interaction of envelope protein with cellular receptors. The fusogenic trimer-of-hairpins conformation is unlikely to be disrupted by 5-Helix, because this hairpin structure involves extremely stable intramolecular interactions (2). Consistent with this assumption, we find that 5-Helix does not bind to recombinant 6-Helix, which mimics the trimer-of-hairpins conformation of gp41.[2] Therefore, our results strongly suggest that the molecular target of 5-Helix is the prehairpin intermediate, a prefusogenic conformation previously inferred from the inhibitory activity of C-peptides (2, 5).

Because this intermediate is a transiently populated species during the membrane fusion process, it has been difficult to determine its structure directly. The analysis of peptide inhibitors, however, provides important insights into its structural features. The binding of the C-peptide DP178 to this intermediate suggests that it contains an exposed trimeric N-peptide coiled coil that has not yet formed a six-helix structure with the adjacent C-peptide region of gp41 (5). Interestingly, the N-peptide $N36^{Mut(e,g)}$, which forms a homotrimer but cannot bind the C-peptide region of gp41, is also a potent inhibitor of gp41-mediated fusion (18). It remains to be shown directly that $N36^{Mut(e,g)}$ binds to the prehairpin intermediate, but this observation raises the possibility that the trimeric N-peptide region of the gp41 prehairpin intermediate undergoes a monomer-trimer equilibrium (18, 27).

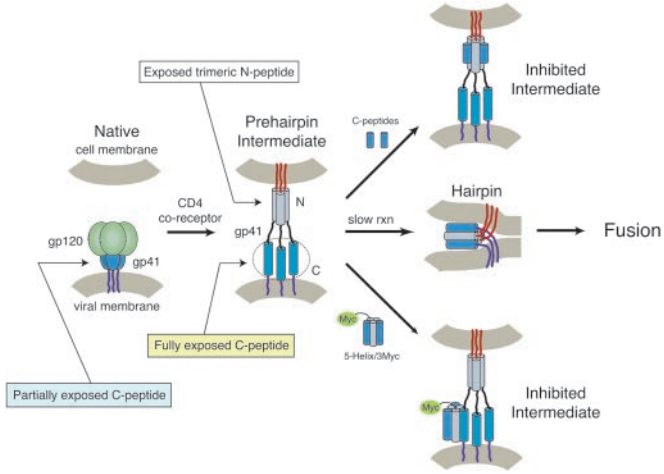

FIG. 6. **A model of HIV-1 membrane fusion and its inhibition.** In the native state (*left panel*) of the trimeric gp120/gp41 complex, the fusion peptide is presumably buried in a hydrophobic pocket within the envelope protein. Little is known about the structure of native gp41, but our results show that the C-peptide region is partially exposed. Upon interaction of gp120 with CD4 and co-receptors on the surface of target cells, gp41 undergoes a conformational change to the prehairpin intermediate state. This transient intermediate has a highly exposed, open structure and is the target for C-peptide and 5-Helix inhibitors. In this prefusogenic state, the N-peptide regions (*gray*) form an exposed trimeric coiled-coil. The C-peptide region (*blue*) is also exposed; it is either in an α-helical conformation or can be readily induced into such a conformation by 5-Helix. We have drawn the prehairpin intermediate with the fusion peptide inserted into the target membrane. However, it should be noted that fusion peptide insertion is probably not essential for exposure of either the N- or C-peptide regions, because binding of DP178 (5) and 5-Helix (Fig. 4) to uncleaved gp160, in which the fusion peptide is expected to be constrained, is activated by cellular receptors. The prehairpin intermediate resolves to the fusion-active hairpin structure when the C peptide region binds to the N peptide trimeric coiled-coil (*right panel*). The diagram was modified from Ref. 2.

Our findings indicate that this prefusogenic conformation also contains C-peptide regions that are exposed enough to allow access of tagged 5-Helix, a 30-kDa protein. Although this exposed C-peptide region almost certainly binds to the 5-Helix protein as an α-helix, we cannot exclude the possibility that it exists in a different conformation in the prehairpin intermediate and is induced into a helical conformation by binding of 5-Helix. Taken together, these results provide a view of the prehairpin intermediate as a largely open structure in which both the N- and C-peptide regions are accessible and thus vulnerable to binding by peptide inhibitors (Fig. 6).

Treatment of HIV-1 virions with sCD4 has been shown to result in gp120 dissociation and the increased binding of several gp41 monoclonal antibodies (4). This observation raises the formal possibility that increased binding of 5-Helix to activated gp41 may likewise reflect exposure of large regions of gp41 because of gp120 shedding. However, we believe that the

[2] T. Koshiba and D. C. Chan, unpublished data.

target of 5-Helix is likely to be a true fusion intermediate, because binding leads to inactivation of gp41 fusion activity. Furthermore, we find that sCD4 leads to increased binding of 5-Helix to uncleaved gp160 (Fig. 4), a result incompatible with the view that gp120 shedding is responsible for 5-Helix binding.

We find that low levels of gp41 binding are observed in the absence of cellular receptors (Fig. 4, *a*, *lanes 3* and *5*, and *b*, *lanes 1* and *2*), implying that the C-peptide region of gp41 is only partially accessible in the absence of activation. This poor accessibility in native gp41 may be due to steric constraints or the adoption of an alternative conformation by the C-peptide region. Alternatively, the low level detected may reflect metastability of the native state of viral envelope proteins (28–30); that is, a small fraction of gp41 molecules at a given time may adopt a prehairpin-like conformation even in the absence of cellular receptors. It is interesting to compare our results with the finding that several monoclonal antibodies (2F5, 4E10, and Z13) directed against the membrane proximal region of gp41 bind better to native gp41 than activated gp41 (31). The epitopes recognized by these antibodies are located slightly C-terminal to the end of the C-peptide, because the 2F5 epitope spans residues 657–670 and the 4E10 epitope spans 671–676. It is likely that these differences in binding preference reflect different conformations recognized by 5-Helix *versus* the monoclonal antibodies. The study of these differences may reveal structural changes in gp41 during the fusion process.

These insights into HIV-1 gp41-mediated membrane fusion will likely also apply to the entry of many other enveloped viruses that have fusion proteins with heptad repeats. Structural studies have revealed that members of the retrovirus, orthomyxovirus, paramyxovirus, and filovirus families contain fusion proteins with a trimer-of-hairpins structure (1, 32). Beyond these structural similarities, the paramyxovirus SV5 fusion protein (F) has been shown to form a transient prehairpin intermediate prior to fusion that can be inhibited by synthetic peptides corresponding to the heptad repeats (33).

Finally, it should be noted that the N- and C-peptide regions of the gp41 prefusogenic intermediate are highly conserved among diverse HIV-1 strains (8, 19). Therefore, it is not surprising that agents targeting these regions have broad neutralizing activity, although the emergence of inhibitor-resistant strains remains a concern (34). Our results should facilitate the development of HIV-1 entry inhibitors and may lead to new vaccine strategies.

Acknowledgments—We gratefully acknowledge Drs. Michael J. Root and Peter S. Kim for providing the p5-Helix and p6-Helix vectors. We also thank Dr. Peter S. Kim for critical reading of the manuscript and members of the Chan lab for helpful comments on the manuscript.

REFERENCES

1. Eckert, D. M., and Kim, P. S. (2001) *Annu. Rev. Biochem.* **70,** 777–810
2. Chan, D. C., and Kim, P. S. (1998) *Cell* **93,** 681–684
3. Sattentau, Q. J., and Moore, J. P. (1991) *J. Exp. Med.* **174,** 407–415
4. Sattentau, Q. J., Moore, J. P., Vignaux, F., Traincard, F., and Poignard, P. (1993) *J. Virol.* **67,** 7383–7393
5. Furuta, R. A., Wild, C. T., Weng, Y., and Weiss, C. D. (1998) *Nat. Struct. Biol.* **5,** 276–279
6. Hoffman, T. L., LaBranche, C. C., Zhang, W., Canziani, G., Robinson, J., Chaiken, I., Hoxie, J. A., and Doms, R. W. (1999) *Proc. Natl. Acad. Sci. U. S. A.* **96,** 6359–6364
7. Dimitrov, A. S., Xiao, X., Dimitrov, D. S., and Blumenthal, R. (2001) *J. Biol. Chem.* **276,** 30335–30341
8. Chan, D. C., Fass, D., Berger, J. M., and Kim, P. S. (1997) *Cell* **89,** 263–273
9. Weissenhorn, W., Dessen, A., Harrison, S. C., Skehel, J. J., and Wiley, D. C. (1997) *Nature* **387,** 426–430
10. Tan, K., Liu, J., Wang, J., Shen, S., and Lu, M. (1997) *Proc. Natl. Acad. Sci. U. S. A.* **94,** 12303–12308
11. Caffrey, M., Cai, M., Kaufman, J., Stahl, S. J., Wingfield, P. T., Covell, D. G., Gronenborn, A. M., and Clore, G. M. (1998) *EMBO J.* **17,** 4572–4584
12. Malashkevich, V. N., Chan, D. C., Chutkowski, C. T., and Kim, P. S. (1998) *Proc. Natl. Acad. Sci. U. S. A.* **95,** 9134–9139
13. Wild, C. T., Shugars, D. C., Greenwell, T. K., McDanal, C. B., and Matthews, T. J. (1994) *Proc. Natl. Acad. Sci. U. S. A.* **91,** 9770–9774
14. Jiang, S., Lin, K., Strick, N., and Neurath, A. R. (1993) *Nature* **365,** 113
15. Chan, D. C., Chutkowski, C. T., and Kim, P. S. (1998) *Proc. Natl. Acad. Sci. U. S. A.* **95,** 15613–15617
16. Eckert, D. M., and Kim, P. S. (2001) *Proc. Natl. Acad. Sci. U. S. A.* **98,** 11187–11192
17. Louis, J. M., Bewley, C. A., and Clore, G. M. (2001) *J. Biol. Chem.* **276,** 29485–29489
18. Bewley, C. A., Louis, J. M., Ghirlando, R., and Clore, G. M. (2002) *J. Biol. Chem.* **277,** 14238–14245
19. Root, M. J., Kay, M. S., and Kim, P. S. (2001) *Science* **291,** 884–888
20. Eckert, D. M., Malashkevich, V. N., Hong, L. H., Carr, P. A., and Kim, P. S. (1999) *Cell* **99,** 103–115
21. Kilby, J. M., Hopkins, S., Venetta, T. M., DiMassimo, B., Cloud, G. A., Lee, J. Y., Alldredge, L., Hunter, E., Lambert, D., Bolognesi, D., Matthews, T., Johnson, M. R., Nowak, M. A., Shaw, G. M., and Saag, M. S. (1998) *Nat. Med.* **4,** 1302–1307
22. Kilby, J. M., Lalezari, J. P., Eron, J. J., Carlson, M., Cohen, C., Arduino, R. C., Goodgame, J. C., Gallant, J. E., Volberding, P., Murphy, R. L., Valentine, F., Saag, M. S., Nelson, E. L., Sista, P. R., and Dusek, A. (2002) *AIDS Res. Hum. Retroviruses* **18,** 685–693
23. Studier, F. W., Rosenberg, A. H., Dunn, J. J., and Dubendorff, J. W. (1990) *Methods Enzymol.* **185,** 60–89
24. Edelhoch, H. (1967) *Biochemistry* **6,** 1948–1954
25. Schagger, H., and von Jagow, G. (1987) *Anal. Biochem.* **166,** 368–379
26. Moulard, M., and Decroly, E. (2000) *Biochim. Biophys. Acta* **1469,** 121–132
27. Caffrey, M., Kaufman, J., Stahl, S., Wingfield, P., Gronenborn, A. M., and Clore, G. M. (1999) *Protein Sci.* **8,** 1904–1907
28. Chen, J., Wharton, S. A., Weissenhorn, W., Calder, L. J., Hughson, F. M., Skehel, J. J., and Wiley, D. C. (1995) *Proc. Natl. Acad. Sci. U. S. A.* **92,** 12205–12209
29. Carr, C. M., Chaudhry, C., and Kim, P. S. (1997) *Proc. Natl. Acad. Sci. U. S. A.* **94,** 14306–14313
30. Chen, J., Lee, K. H., Steinhauer, D. A., Stevens, D. J., Skehel, J. J., and Wiley, D. C. (1998) *Cell* **95,** 409–417
31. Zwick, M. B., Labrijn, A. F., Wang, M., Spenlehauer, C., Saphire, E. O., Binley, J. M., Moore, J. P., Stiegler, G., Katinger, H., Burton, D. R., and Parren, P. W. (2001) *J. Virol.* **75,** 10892–10905
32. Skehel, J. J., and Wiley, D. C. (1998) *Cell* **95,** 871–874
33. Russell, C. J., Jardetzky, T. S., and Lamb, R. A. (2001) *EMBO J.* **20,** 4024–4034
34. Wei, X., Decker, J. M., Liu, H., Zhang, Z., Arani, R. B., Kilby, J. M., Saag, M. S., Wu, X., Shaw, G. M., and Kappes, J. C. (2002) *Antimicrob. Agents Chemother.* **46,** 1896–1905